



Sound radiation of orthogonally stiffened laminated composite plates under airborne and structure borne excitations



C. Shen^{a,b}, F.X. Xin^{a,*}, L. Cheng^b, T.J. Lu^{a,*}

^a State Key Laboratory for Mechanical Structure Strength and Vibration, School of Aerospace, Xi'an Jiaotong University, Xi'an 710049, PR China

^b Department of Mechanical Engineering, The Hong Kong Polytechnic University, Hung Hom, Kowloon, Hong Kong SAR, PR China

ARTICLE INFO

Article history:

Received 8 December 2012

Received in revised form 1 May 2013

Accepted 2 May 2013

Available online 20 May 2013

Keywords:

C. Laminate theory

C. Sandwich structures

C. Modeling

D. Acoustic emission

ABSTRACT

An analytical periodic model is developed to predict the radiation of sound from orthogonally stiffened laminated composite plates under airborne and structure borne excitations. Whilst a layerwise shear deformable theory is used to describe the vibration of the base plate, both the force and moment coupling between the stiffeners and the base plate are considered on basis of flexural-torsion coupling equations. The periodic governing equations are solved using Fourier transformation method. The validity and feasibility of the model is verified by comparing theoretical predictions with existing numerical and experimental results. Numerical discussions with the model demonstrate the significant influence of both flexural-extension and flexural-torsion coupling upon acoustic radiation from un-stiffened composite plate, which depends on material properties, geometrical parameters and frequency.

© 2013 Elsevier Ltd. All rights reserved.

1. Introduction

As laminated, fiber-reinforced composite structures are increasingly exploited in a wide range of engineering applications [1], stiffeners are commonly used to further reinforce the laminated composite structure. To deal with stiffened structures, a most straightforward way [2] is to equivalent the whole structure as an orthotropic uniform plate if the mechanical wavelengths are greater than stiffener spacing. To describe the coupling forces between the stiffeners and the base plate, the stiffeners are conveniently replaced with lumped mass and spring [3]. More accurately, Langley and Heron [4] have given general coupling matrix at plate/beam junction, which can be extended to predict reactive forces by stiffeners. To solve the governing equations, Mead and Pujara [3] developed the method of space harmonic expansion, which has been developed to investigate a variety of periodically stiffened structures [5–7]. Employing the technique of Fourier transform [8], Mace [9,10] investigated the response of plates with parallel and orthogonal stiffeners under fluid loading, whereas Takahashi [11] studied sound radiation from double-leaf structures with periodical connections. Both of the two approaches described above transform the governing equations into infinite sets of simultaneous algebraic equations and then truncate these into a finite range for numerical solutions.

In comparison with the isotropic material made structures, the laminated composite material made structure significantly increases the complexity of the theoretical modeling. To deal with the laminated composite structure, Yin et al. [12] extended Mace's model [9] to unidirectional stiffened laminated composite plate based on the classical laminated composite plate theory (CLPT), in which the bending motion of metallic stiffeners has been accounted for. Also based on CLPT theory, Legault et al. [13] explored the effect of finite dimensions by comparing the spatially windowing periodic model with the Rayleigh–Ritz method. It is concluded that the periodic theory is inappropriate when the bending wavelength is smaller than the stiffener spacing. There also exists such a restriction in the present paper since the periodic theory is used here. Recently, a first order shear deformation theory (FSDT) is employed by Mejadi et al. [14] to consider the transverse shear strain of base plate, where the in plane motion of stiffeners has been taken into account. Whereas, the governing equations for stiffeners only apply to thin-walled isotropic beam (or uncoupled composite case) while not the general composite beam.

To develop a more accurate theoretical model, a layerwise shear deformable theory is applied to model the vibration of the laminate composite base plate, and the shear deformable beam theory is utilized to model the vibration of arbitrary thin-walled composite beam stiffeners. Note that the single-layer theories (e.g. CLPT or FSDT) used by previous researchers remain acceptable for thin bare plate, which probably induce significant deviations for thicker and stiffened plates. Different from the existing studies, numerical discussions specially focus on the flexural-extension and the flexural-torsion coupling effects caused by the material anisotropy of

* Corresponding authors. Tel.: +86 29 82665600; fax: +86 29 83234781.

E-mail addresses: fengxian.xin@gmail.com (F.X. Xin), tjlu@mail.xjtu.edu.cn (T.J. Lu).

composite base plate, as well as the flexural-torsion coupling effect due to the geometrical anisotropy of the stiffeners.

2. Mathematical formulation

With reference to Fig. 1, consider an infinite laminated composite plate reinforced by orthogonal line stiffeners (without plate like behavior) along the lines $x = ml_x$ and $y = nl_y$, with (m, n) representing integers and (l_x, l_y) denoting spacing respectively. The origin of the Cartesian coordinates is located at the junction of the orthogonal stiffeners. The structure is loaded by acoustic fluid on one side, i.e., the side without stiffeners. Under a layerwise shear deformable theory [15], the discrete laminated model can express the displacements for the i th layer of the composite base plate as:

$$\begin{cases} u^i(x, y, z, t) = u_0^i(x, y, t) + z\phi_x^i(x, y, t) \\ v^i(x, y, z, t) = v_0^i(x, y, t) + z\phi_y^i(x, y, t) \\ w^i(x, y, z, t) = w_0^i(x, y, t) \end{cases} \quad (1)$$

where (u_0^i, v_0^i, w_0^i) are the displacements of the plate along (x, y, z) coordinate directions in the mid-plane of each layer, and (ϕ_x^i, ϕ_y^i) denote the rotation displacements of the plate about the (y, x) directions, respectively.

The Euler–Lagrange equations of the system incorporating the reaction forces due to the stiffeners may be written as:

$$\begin{aligned} \frac{\partial N_{xx}^i}{\partial x} + \frac{\partial N_{xy}^i}{\partial y} - I_0^i \frac{\partial^2 u_0^i}{\partial t^2} - I_1^i \frac{\partial^2 \phi_x^i}{\partial t^2} + F_x^i - F_x^{i-1} \\ = f_x^i - \delta_{il} \left[\sum_{m \in \mathbb{Z}} F_{xx} \delta(x - ml_x) + \sum_{n \in \mathbb{Z}} F_{yx} \delta(y - nl_y) \right] \end{aligned} \quad (2)$$

$$\begin{aligned} \frac{\partial N_{yy}^i}{\partial y} + \frac{\partial N_{xy}^i}{\partial x} - I_0^i \frac{\partial^2 v_0^i}{\partial t^2} - I_1^i \frac{\partial^2 \phi_y^i}{\partial t^2} + F_y^i - F_y^{i-1} \\ = f_y^i - \delta_{il} \left[\sum_{m \in \mathbb{Z}} F_{xy} \delta(x - ml_x) + \sum_{n \in \mathbb{Z}} F_{yy} \delta(y - nl_y) \right] \end{aligned} \quad (3)$$

$$\begin{aligned} \frac{\partial Q_y^i}{\partial y} + \frac{\partial Q_x^i}{\partial x} - I_0^i \frac{\partial^2 w_0^i}{\partial t^2} + F_z^i - F_z^{i-1} \\ = P_{exc}^i - P_a^i - \delta_{il} \left[\sum_{m \in \mathbb{Z}} F_{xz} \delta(x - ml_x) + \sum_{n \in \mathbb{Z}} F_{yz} \delta(y - nl_y) \right] \end{aligned} \quad (4)$$

$$\begin{aligned} \frac{\partial M_{xy}^i}{\partial x} + \frac{\partial M_{yx}^i}{\partial y} - Q_y^i - I_1^i \frac{\partial^2 u_0^i}{\partial t^2} - I_2^i \frac{\partial^2 \phi_x^i}{\partial t^2} + \frac{h^i}{2} F_x^i + \frac{h^i}{2} F_x^{i-1} \\ = -\delta_{il} \left[\sum_{m \in \mathbb{Z}} M_x \delta(x - ml_x) \right] \end{aligned} \quad (5)$$

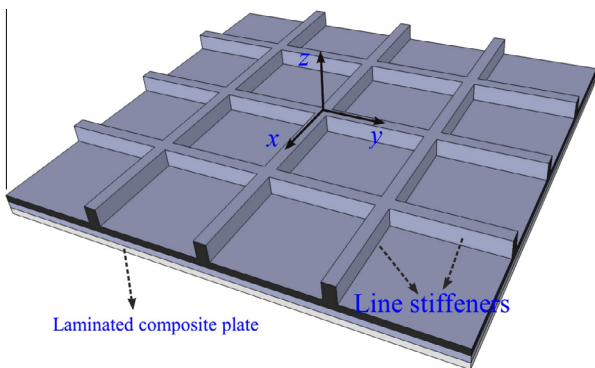


Fig. 1. Laminated composite plate reinforced by orthogonal line stiffeners.

$$\begin{aligned} \frac{\partial M_{xy}^i}{\partial x} + \frac{\partial M_{yx}^i}{\partial y} - Q_y^i - I_1^i \frac{\partial^2 u_0^i}{\partial t^2} - I_2^i \frac{\partial^2 \phi_x^i}{\partial t^2} + \frac{h^i}{2} F_x^i + \frac{h^i}{2} F_x^{i-1} \\ = -\delta_{il} \left[\sum_{n \in \mathbb{Z}} M_y \delta(y - nl_y) \right] \end{aligned} \quad (6)$$

where P_{exc}^i denotes a general excitation (e.g. airborne or structure borne excitations), P_a^i is the radiated acoustic pressure in the fluid; f_x^i and f_y^i are external forces acting in the plane of the base plate; $(F_{x\epsilon}, F_{y\epsilon})$ $\{\epsilon = x, y, z\}$ and (M_x, M_y) are the coupling forces and reactive torsion moments between the stiffeners and the base plate. The total number of interlayer forces (F_x^i, F_y^i, F_z^i) is $3(N-1)$, where N is the number of layers. δ_{il} is the Kronecker delta symbol. Then, total $5N + 3(N-1)$ variables can be grouped into two vectors including the displacement vector $\{\mathbf{U}\}$ and the interlayer force vector $\{\mathbf{F}\}$:

$$\begin{aligned} \{\mathbf{U}\} = \{u_0^1, v_0^1, w_0^1, \phi_x^1, \phi_y^1, u_0^2, v_0^2, w_0^2, \phi_x^2, \phi_y^2, \dots, u_0^N, v_0^N, w_0^N, \phi_x^N, \phi_y^N\}^T, \\ \{\mathbf{F}\} = \{F_x^1, F_y^1, F_z^1, F_x^2, F_y^2, F_z^2, \dots, F_x^{N-1}, F_y^{N-1}, F_z^{N-1}\}^T. \end{aligned} \quad (7)$$

Further, I_0^i, I_1^i and I_2^i are the mass moments of inertia, defined by:

$$(I_0^i, I_1^i, I_2^i) = \int_{z_b^i}^{z_t^i} (1, z, z^2) \rho^i dz \quad (8)$$

where ρ^i and $z_b^i(z_t^i)$ denotes the mass density and coordinate of bottom (top) of the i th layer of the laminated composite plate, respectively. Interlayer displacement continuity condition requires:

$$u_0^i + z_i \phi_x^i = u_0^{i+1} + z_i \phi_x^{i+1}, v_0^i + z_i \phi_y^i = v_0^{i+1} + z_i \phi_y^{i+1}, w_0^i = w_0^{i+1} \quad (9)$$

In all, the $5N + 3(N-1)$ variables (Eq. (7)) correspond to $5N$ dynamic equilibrium equations (Eqs. (2)–(6)) and $3(N-1)$ displacement continuity equations (Eq. (9)). Notice that the present layerwise shear deformable theory model can be degraded into the FSDT model if the number of total layers is set to be one.

To solve the governing equations, the method of Space Fourier Transformation (SFT) is employed here for its capability to consider the effects of fluid loading and infinite periodic structures, so that:

$$\tilde{w}(\alpha, \beta) = \int_{-\infty}^{+\infty} \int_{-\infty}^{+\infty} w(x, y) e^{i(\alpha x + \beta y)} dx dy, \quad (10)$$

$$w(x, y) = \frac{1}{4\pi^2} \int_{-\infty}^{+\infty} \int_{-\infty}^{+\infty} \tilde{w}(\alpha, \beta) e^{-i(\alpha x + \beta y)} d\alpha d\beta \quad (11)$$

Transforming Eqs. (2)–(6) and Eq. (9) then leads to:

$$([A_2] + i[A_1] - [A_0])\{\tilde{e}\} = \{\tilde{P}_f\} - \{\tilde{P}_{F_x}\} - \{\tilde{P}_{F_y}\} \quad (12)$$

where $i = \sqrt{-1}$, the coefficient matrixes $([A_0], [A_1], [A_2])$ are defined by Ghinet and Atalla [15]. The coupling sound pressure $\tilde{P}_a(\alpha, \beta, 0) = -\omega^2 \rho_0 \tilde{w}(\alpha, \beta) / \sqrt{\alpha^2 + \beta^2 - \omega^2/c_0^2}$ (c_0 is the speed of sound, ρ_0 is the density of fluid) at fluid–panel interface can be easily joined into the coefficient matrixes. Then, the hybrid variables vector, excitation forces vector, reaction forces between the base plate and the stiffeners can be written as:

$$\begin{aligned} \{\tilde{e}\} = \{\tilde{\mathbf{U}}^T, \tilde{\mathbf{F}}^T\}^T, \{\tilde{P}_f\} = \{\tilde{f}_x^1, \tilde{f}_y^1, \tilde{P}_{exc}^1, 0, 0, \dots, \tilde{f}_x^N, \tilde{f}_y^N, \tilde{P}_{exc}^N, 0, 0\}^T, \\ \{\tilde{P}_{F_x}\} = \{\tilde{F}_{xx}, \tilde{F}_{xy}, \tilde{F}_{xz}, \tilde{M}_x, \underbrace{0, \dots, 0}_{8N-7}\}^T, \{\tilde{P}_{F_y}\} = \{\tilde{F}_{yx}, \tilde{F}_{yy}, \tilde{F}_{yz}, 0, \tilde{M}_y, \underbrace{0, \dots, 0}_{8N-8}\}^T. \end{aligned} \quad (13)$$

2.1. Reactive forces by stiffeners

As above mentioned in Section 1, the existing theoretical works about stiffened composite plate could only consider isotropic or uncoupled composite beam stiffeners. While, the shear deformable

beam theory that can handle arbitrary thin-walled composite beams is introduced here [16]:

$$\langle Q \rangle = \begin{bmatrix} q_x \\ q_y \\ q_z \\ m_x \\ m_y \\ m_z \end{bmatrix} = \begin{bmatrix} a_{11} & a_{12} & a_{13} & a_{14} & a_{15} & a_{16} \\ a_{21} & a_{22} & a_{23} & a_{24} & a_{25} & a_{26} \\ a_{31} & a_{32} & a_{33} & a_{34} & a_{35} & a_{36} \\ a_{41} & a_{42} & a_{43} & a_{44} & a_{45} & a_{46} \\ a_{51} & a_{52} & a_{53} & a_{54} & a_{55} & a_{56} \\ a_{61} & a_{62} & a_{63} & a_{64} & a_{65} & a_{66} \end{bmatrix} \begin{bmatrix} u \\ v \\ w \\ \psi_x \\ \psi_y \\ \psi_z \end{bmatrix} = [A] \langle a \rangle \quad (14)$$

where $\langle Q \rangle$, $\langle a \rangle$, $[A]$ represent force vector, displacement vector and coefficient matrix, respectively. Remarkably, it is shown that various coupling effects may take place among these six unknown displacements variables. In the present paper, attention is paid to the flexural-torsion coupling effect due to the geometric rather than the material anisotropy of stiffeners. Then, the non-zero coefficients a_{ij} for C shape beam in y-direction are given:

$$a_{11} = EI_z \frac{\partial^4}{\partial y^4} - m_0 \omega^2; \quad a_{22} = -EA \frac{\partial^2}{\partial y^2} - m_0 \omega^2; \quad a_{33} = EI_x \frac{\partial^4}{\partial y^4} - m_0 \omega^2; \\ a_{35} = a_{53} = m_0 x_c \omega^2; \quad a_{55} = EI_w \frac{\partial^4}{\partial y^4} - GJ \frac{\partial^2}{\partial y^2} + (m_p + m_2) \omega^2. \quad (15)$$

where the definitions of all these constants can be found in Lee and Kim's paper [17]. All the damping effects in the present work are assumed to be structural damping and expressed in the form of complex Young's modulus. The relationship between the beam reaction forces ($\langle Q \rangle$) and base plate reaction forces ($\langle F \rangle$) can be written as [2]:

$$\langle Q \rangle = \begin{bmatrix} q_x \\ q_y \\ q_z \\ m_x \\ m_y \\ m_z \end{bmatrix} = \begin{bmatrix} 1 & 0 & 0 & 0 \\ 0 & 1 & 0 & 0 \\ 0 & 0 & 1 & 0 \\ 0 & z_c & 0 & 0 \\ -z_c & \omega^* \frac{\partial}{\partial y} & x_c & 1 \\ x_c & 0 & 0 & 0 \end{bmatrix} \begin{bmatrix} F_{xx} \\ F_{xy} \\ F_{xz} \\ M_x \end{bmatrix} = [R] \langle F \rangle \quad (16)$$

where the point (x_c, z_c) denotes the line junction between stiffeners and base plate with respect to shear center of stiffeners, ω^* represents the warping function of stiffeners and $\frac{\partial}{\partial y}$ denotes the first-order derivative with respect to y . Then, displacement continuity between the beam displacement $\langle a \rangle$ and the base plate displacement $\langle b \rangle$ requires:

$$\langle b \rangle = [u_0^1, v_0^1, w_0^1, \phi_y^1]^T = [R]^T \langle a \rangle \quad (17)$$

Notice that the flexural-torsion coupling effect of eccentric stiffeners has been reflected in the relation matrix $\langle R \rangle$ explicitly. Combining Eqs. (15)–(17), the reactive forces of stiffeners are related to the plate displacement as:

$$\langle F \rangle = ([R]^T [A]^{-1} [R])^{-1} \langle b \rangle \quad (18)$$

To solve the Dirac function appearing in Eqs. (2)–(6), the Poisson formula is employed [10,11]:

$$\sum_{m \in \mathbb{Z}} \delta(x - ml_x) = \frac{1}{l_x} \sum_{n \in \mathbb{Z}} \exp\left(\frac{2in\pi x}{l_x}\right) \quad (19)$$

Upon incorporating Eqs. (18), (19) and introducing the definition ($\alpha_m = \alpha + 2m\pi/l_x$, $\beta_n = \beta + 2n\pi/l_y$), The transform of the coupling forces between the stiffeners and the base plate along the y -direction is obtained as:

$$\langle \tilde{F}_x \rangle = \begin{bmatrix} \tilde{F}_{xx} \\ \tilde{F}_{xy} \\ \tilde{F}_{xz} \\ \tilde{M}_x \end{bmatrix} = \begin{bmatrix} \tilde{z}_x^{11} & \tilde{z}_x^{12} & \tilde{z}_x^{13} & \tilde{z}_x^{14} & 0 \\ \tilde{z}_x^{21} & \tilde{z}_x^{22} & \tilde{z}_x^{23} & \tilde{z}_x^{24} & 0 \\ \tilde{z}_x^{31} & \tilde{z}_x^{32} & \tilde{z}_x^{33} & \tilde{z}_x^{34} & 0 \\ \tilde{z}_x^{41} & \tilde{z}_x^{42} & \tilde{z}_x^{43} & \tilde{z}_x^{44} & 0 \end{bmatrix} \begin{bmatrix} \sum_{m \in \mathbb{Z}} \tilde{u}_0^1(\alpha_m, \beta) \\ \sum_{m \in \mathbb{Z}} \tilde{v}_0^1(\alpha_m, \beta) \\ \sum_{m \in \mathbb{Z}} \tilde{w}_0^1(\alpha_m, \beta) \\ \sum_{m \in \mathbb{Z}} \tilde{\phi}_x^1(\alpha_m, \beta) \\ \sum_{m \in \mathbb{Z}} \tilde{\phi}_y^1(\alpha_m, \beta) \end{bmatrix} \quad (20)$$

where \tilde{z}_x^{ij} ($i, j = 1 \sim 4$) represents the transformed coefficient matrix elements. Similarly, the reactive forces by stiffeners along x -direction are expressed as:

$$\langle \tilde{F}_y \rangle = \begin{bmatrix} \tilde{F}_{yx} \\ \tilde{F}_{yy} \\ \tilde{F}_{yz} \\ \tilde{M}_y \end{bmatrix} = \begin{bmatrix} \tilde{z}_y^{11} & \tilde{z}_y^{12} & \tilde{z}_y^{13} & 0 & \tilde{z}_y^{14} \\ \tilde{z}_y^{21} & \tilde{z}_y^{22} & \tilde{z}_y^{23} & 0 & \tilde{z}_y^{24} \\ \tilde{z}_y^{31} & \tilde{z}_y^{32} & \tilde{z}_y^{33} & 0 & \tilde{z}_y^{34} \\ \tilde{z}_y^{41} & \tilde{z}_y^{42} & \tilde{z}_y^{43} & 0 & \tilde{z}_y^{44} \end{bmatrix} \begin{bmatrix} \sum_{n \in \mathbb{Z}} \tilde{u}_0^1(\alpha, \beta_n) \\ \sum_{n \in \mathbb{Z}} \tilde{v}_0^1(\alpha, \beta_n) \\ \sum_{n \in \mathbb{Z}} \tilde{w}_0^1(\alpha, \beta_n) \\ \sum_{n \in \mathbb{Z}} \tilde{\phi}_x^1(\alpha, \beta_n) \\ \sum_{n \in \mathbb{Z}} \tilde{\phi}_y^1(\alpha, \beta_n) \end{bmatrix} \quad (21)$$

Combining Eqs. (12), (20), and (21), the resultant governing equations in wavenumber domain can thence be given as:

$$\begin{bmatrix} \tilde{u}_0^1(\alpha, \beta) \\ \tilde{v}_0^1(\alpha, \beta) \\ \tilde{w}_0^1(\alpha, \beta) \\ \tilde{\phi}_x^1(\alpha, \beta) \\ \tilde{\phi}_y^1(\alpha, \beta) \end{bmatrix} = L_{5 \times 5}^* \begin{bmatrix} \tilde{f}_x \\ \tilde{f}_y \\ \tilde{p}_{exc} \\ 0 \\ 0 \end{bmatrix} - L_{5 \times 5}^* \begin{bmatrix} \tilde{z}_x^{11} & \tilde{z}_x^{12} & \tilde{z}_x^{13} & \tilde{z}_x^{14} & 0 \\ \tilde{z}_x^{21} & \tilde{z}_x^{22} & \tilde{z}_x^{23} & \tilde{z}_x^{24} & 0 \\ \tilde{z}_x^{31} & \tilde{z}_x^{32} & \tilde{z}_x^{33} & \tilde{z}_x^{34} & 0 \\ \tilde{z}_x^{41} & \tilde{z}_x^{42} & \tilde{z}_x^{43} & \tilde{z}_x^{44} & 0 \\ 0 & 0 & 0 & 0 & 0 \end{bmatrix} \begin{bmatrix} \sum_{m \in \mathbb{Z}} \tilde{u}_0^1(\alpha_m, \beta) \\ \sum_{m \in \mathbb{Z}} \tilde{v}_0^1(\alpha_m, \beta) \\ \sum_{m \in \mathbb{Z}} \tilde{w}_0^1(\alpha_m, \beta) \\ \sum_{m \in \mathbb{Z}} \tilde{\phi}_x^1(\alpha_m, \beta) \\ \sum_{m \in \mathbb{Z}} \tilde{\phi}_y^1(\alpha_m, \beta) \end{bmatrix} \\ - L_{5 \times 5}^* \begin{bmatrix} \tilde{z}_y^{11} & \tilde{z}_y^{12} & \tilde{z}_y^{13} & 0 & \tilde{z}_y^{14} \\ \tilde{z}_y^{21} & \tilde{z}_y^{22} & \tilde{z}_y^{23} & 0 & \tilde{z}_y^{24} \\ \tilde{z}_y^{31} & \tilde{z}_y^{32} & \tilde{z}_y^{33} & 0 & \tilde{z}_y^{34} \\ 0 & 0 & 0 & 0 & 0 \\ \tilde{z}_y^{41} & \tilde{z}_y^{42} & \tilde{z}_y^{43} & 0 & \tilde{z}_y^{44} \end{bmatrix} \begin{bmatrix} \sum_{n \in \mathbb{Z}} \tilde{u}_0^1(\alpha, \beta_n) \\ \sum_{n \in \mathbb{Z}} \tilde{v}_0^1(\alpha, \beta_n) \\ \sum_{n \in \mathbb{Z}} \tilde{w}_0^1(\alpha, \beta_n) \\ \sum_{n \in \mathbb{Z}} \tilde{\phi}_x^1(\alpha, \beta_n) \\ \sum_{n \in \mathbb{Z}} \tilde{\phi}_y^1(\alpha, \beta_n) \end{bmatrix} \quad (22)$$

where $L_{5 \times 5}^*$ denotes the first five lines and columns of the inversion stiffness matrix in Eq. (12). To solve the coupling unknowns, two sets of intermediate variable are introduced here as:

$$\begin{cases} \xi_m(\alpha_m, \beta) = \left[\sum_{n \in \mathbb{Z}} \tilde{u}_0^1(\alpha_m, \beta_n), \sum_{n \in \mathbb{Z}} \tilde{v}_0^1(\alpha_m, \beta_n), \sum_{n \in \mathbb{Z}} \tilde{w}_0^1(\alpha_m, \beta_n), \sum_{n \in \mathbb{Z}} \tilde{\phi}_x^1(\alpha_m, \beta_n), \sum_{n \in \mathbb{Z}} \tilde{\phi}_y^1(\alpha_m, \beta_n) \right]^T \\ \xi_n(\alpha, \beta_n) = \left[\sum_{m \in \mathbb{Z}} \tilde{u}_0^1(\alpha_m, \beta_n), \sum_{m \in \mathbb{Z}} \tilde{v}_0^1(\alpha_m, \beta_n), \sum_{m \in \mathbb{Z}} \tilde{w}_0^1(\alpha_m, \beta_n), \sum_{m \in \mathbb{Z}} \tilde{\phi}_x^1(\alpha_m, \beta_n), \sum_{m \in \mathbb{Z}} \tilde{\phi}_y^1(\alpha_m, \beta_n) \right]^T \end{cases} \quad (23)$$

Notice that the definition $(\xi(\alpha, \beta) = [\tilde{u}_0^1(\alpha, \beta), \tilde{v}_0^1(\alpha, \beta), \tilde{w}_0^1(\alpha, \beta), \tilde{\phi}_x^1(\alpha, \beta), \tilde{\phi}_y^1(\alpha, \beta)]^T, \alpha_m = \alpha + 2m\pi/l_x, \beta_n = \beta + 2n\pi/l_y)$, the intermediate variables have the periodicity properties:

$$\xi_m(\alpha_m, \beta) = \xi_m(\alpha_m, \beta_n), \xi_n(\alpha, \beta_n) = \xi_n(\alpha_m, \beta_n) \quad (24)$$

Once these intermediate variables of Eq. (23) are determined, the displacements in wavenumber domain can be obtained using Eq. (22). Given the definition of intermediate variables in Eq. (23) and their periodicity property shown in Eq. (24), summing Eq. (22) over all m (or n) values yields:

$$\begin{cases} \xi_n(\alpha, \beta_n) = \sum_{m \in \mathbb{Z}} \tilde{P}_f(\alpha_m, \beta_n) + \sum_{m \in \mathbb{Z}} S_1(\alpha_m, \beta_n) \xi_n(\alpha, \beta_n) + \sum_{m \in \mathbb{Z}} S_2(\alpha_m, \beta_n) \xi_m(\alpha_m, \beta_n) \\ \xi_m(\alpha_m, \beta) = \sum_{n \in \mathbb{Z}} \tilde{P}_f(\alpha_m, \beta_n) + \sum_{n \in \mathbb{Z}} S_1(\alpha_m, \beta_n) \xi_n(\alpha, \beta_n) + \sum_{n \in \mathbb{Z}} S_2(\alpha_m, \beta_n) \xi_m(\alpha_m, \beta_n) \end{cases} \quad (25)$$

where $\tilde{P}_f(\alpha, \beta)$, $S_1(\alpha, \beta)$ and $S_2(\alpha, \beta)$ correspond to the coefficient matrix in Eq. (22). Here, the sum-indices (m, n) are restricted to have finite values, i.e., $m = -\hat{m}$ to \hat{m} and $n = -\hat{n}$ to \hat{n} , thus Eq. (25) forms a system of $2(\hat{m} + \hat{n} + 1)$ linear equations for determining the intermediate variables $\xi(\alpha_m, \beta)$ (total $2\hat{m} + 1$) and $\xi(\alpha, \beta_n)$ (total $2\hat{n} + 1$). The convergence criteria said that once the solution was convergent at a given frequency, it is also convergent for all frequency lower than that [18]. Therefore, the convergence check is performed at the highest frequency 10 kHz of interest here, and it is found that the sum-indices taking values $\hat{m} = \hat{n} = 15$ can ensure the convergence of the results within the error bound of 0.5 dB.

2.2. Far field radiated sound pressure and sound transmission loss

Following the standard procedure of stationary phase [19], the far field acoustic radiation in spherical coordinates can be obtained if neglecting the radiation from stiffeners:

$$P(R, \theta, \phi) = -\rho_0 \omega^2 \tilde{w}_0^1(\alpha_0, \beta_0) \exp(-ik_0 R) / 2\pi R \quad (26)$$

where $\alpha_0 = k_0 \sin \theta \cos \phi$, $\beta_0 = k_0 \sin \theta \sin \phi$, ρ_0 is the density of fluid, $k_0 = \omega/c_0$ is acoustic wavenumber, (R, θ, ϕ) are the selected spherical coordinates. The high frequency asymptote of the far field sound pressure $P_r = \rho_0 Q \exp(-ik_0 R) / 2\pi m_p R$ (m_p is the surface density of base plate, Q is the amplitude of imposed point force) radiated by an unstiffened plate is selected here as a Ref. [10]. Then, the far field sound pressure can be expressed by sound pressure level (SPL = $20 \log_{10}(P/P_r)$) in decibel scales (dB).

Assuming both sides of the plate emerged in fluids and excited by sound pressure P_i , the sound transmission problem can also be handled by the above formulated model based on the layerwise shear deformable theory, the incident sound intensity is defined as $W_i = \frac{1}{2} (|P_i|^2 \cos \varphi / \rho_0 c_0)$, where φ is the sound incidence angle. The transmitted sound intensity is given in wavenumber domain as [20]

$$W_t = \frac{\rho_0 \omega^3}{8\pi^2} \sum_{(\alpha_m^2 + \beta_n^2) < (\omega/c_0)^2} \frac{|\tilde{w}_0^1(\alpha_m, \beta_n)|^2}{\sqrt{(\omega/c_0)^2 - \alpha_m^2 - \beta_n^2}} \quad (27)$$

Then, sound transmission loss (STL) is expressed by the formula $STL = -10 \log_{10}(W_t/W_i)$. This theoretical model for predicting STL of infinite structure can also take account of finite size effect approximately by applying the windowing technique. Whereas, it will be cumbersome to execute the windowing process in wavenumber field following the classical spatial windowing method [21]. Alternatively, a finite radiation efficiency σ_f [22] is adopted here to replace the infinite radiation efficiency in the calculation of the transmitted sound intensity, which can be written as:

$$W_t = \frac{\rho_0 c_0 \omega^2}{8\pi^2} \sum_{(\alpha_m^2 + \beta_n^2) < k_0^2} \sigma_f(\alpha_m, \beta_n, \omega) |\tilde{w}_0^1(\alpha_m, \beta_n)|^2 \quad (28)$$

3. Results and discussion

In this section, numerical calculations based on theoretical formulations presented above are performed to explore the vibroacoustic characteristics of infinite laminated composite plates stiffened by orthogonal C shape stiffeners. Unless otherwise stated, the following material and geometry parameters are used as follows. The base plate is made of composite material with modulus $E_1 = 150$ GPa, $E_2 = 9.0$ GPa, $G_{12} = G_{13} = 7.1$ GPa, $G_{23} = 2.5$ GPa, density $\rho = 1600$ kg/m³, and thickness $h = 0.012$ m. The acoustic fluid has a density $\rho_0 = 1000$ kg/m³ with sound speed $c_0 = 1500$ m/s. Parameters of C-shape stiffeners are chosen with modulus $E = 195$ GPa, density $\rho_1 = 7700$ kg/m³, web width $b_1 = 0.02$ m, flange width $b_2 = 0.02$ m, thickness $h_1 = 0.001$ m, and stiffener spacing $l_x = l_y = 0.2$ m.

3.1. Validation of theoretical modeling

To verify the validity of the present theoretical model, the predictions are compared with existing theoretical results of Mace [10] for sound radiation of orthogonally stiffened uniform plates, as shown in Fig. 2. To indicate the advantage of the layerwise shear deformable theory based model, the predictions for the structures of the one layer and three layer configurations (with the same thickness) are also included in Fig. 2. Note that whilst Mace adopted the Kirchhoff thin plate theory to describe the base plate, the present model applying to the one layer configuration is actually degraded to the first order shear deformation theory (FSDT). The comparison of Fig. 2 demonstrates that the present results agree excellently well with Mace's results over a wide frequency range. The discrepancies appearing approximately above 7000 Hz are mainly attributed to the fact that the torsion moments of the stiffeners are considered in the present theoretical model but not in Mace's model, and another reason lies on the different plate theory. Moreover, it is interesting to note that, there exists significant difference between two different configurations for stiffened cases while no distinction is observed for unstiffened cases. This actually demonstrates the advantage of the present layerwise shear deformable theory based model, that is, it is necessary to adopt the more accurate theory (i.e., the layerwise shear deformable theory) to model the stiffened composite plates.

To further check the applicability of the present model, the infinite model predictions and the finite model predictions (i.e., the finite radiation efficiency is applied) are both compared with the published experimental results [23] for the sound transmission

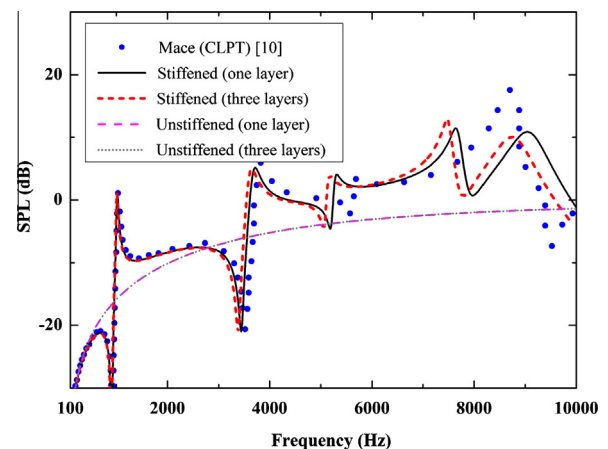


Fig. 2. Present model predictions compared with theoretical results of Mace [10] for sound radiation of orthogonally stiffened uniform plate.

loss (1/3 octave) of unidirectional all metallic stiffened panel as shown in Fig. 3. In this experiment, the size of the 4 mm thick aluminum base panel is 2.73 m by 3.43 m, and the periodic aluminum stiffeners are spaced 40 mm apart. Again, the present model predictions are in good agreement with the experimental results especially in the coincidence region. The theoretical model with the finite radiation efficiency applied shows superiority over the infinite model in terms of the excellent agreements with experimental results over the whole frequency range, particularly in the low frequency region.

3.2. Flexural-extension coupling effect of composite bare plate

First, sound radiation from unstiffened laminated composite plates excited by a transverse point force is considered, which has been modeled by Yin and Cui [24] amongst others. To quantify the flexural-extension coupling effect, Fig. 4 presents the predicted sound pressure levels for two typical lamination schemes: symmetric $[75^\circ/60^\circ/45^\circ]_{\text{sym}}$ and anti-symmetric plies $[75^\circ/60^\circ/45^\circ]_{\text{antisym}}$. The predictions by Yin and Cui [24] based on CLPT are also included for comparison.

Yin and Cui [24] demonstrated that the influence of different lamination schemes upon the SPL of a composite plate is negligible, as shown in Fig. 4. However, if the thickness of a single ply is increased from 1.5 mm to 2 mm (other parameters remain unchanged), there exists a noticeable discrepancy between the present predictions and Yin and Cui’s results especially in the high frequency regime. This actually implies that the layerwise shear deformable theory applied here is more accurate than the classical laminated plate theory (CLPT) adopted by Yin and Cui [24] for dealing with relatively thick composite plates for which the flexural-extension coupling effect can be well demonstrated. Also, the symmetric lamination scheme is found to produce stronger radiation pressure than the antisymmetric one. This is considered reasonable because flexural-extension coupling is absent in the symmetric scheme and hence less energy is converted from bending wave to longitudinal wave. Whereas, the coincidence of all four curves in the low frequency regime (<3000 Hz) of Fig. 4 should be attributed to the fact that the identical heavy fluid (i.e., water considered here) dominates the low-frequency dynamic response of composite plates [25].

To investigate further the flexural-extension coupling effect, Fig. 5 presents the radiated sound pressure level of symmetrical as well as anti-symmetrical laminates excited by an in-plane point force. It is seen that, owing to the flexural-extension coupling

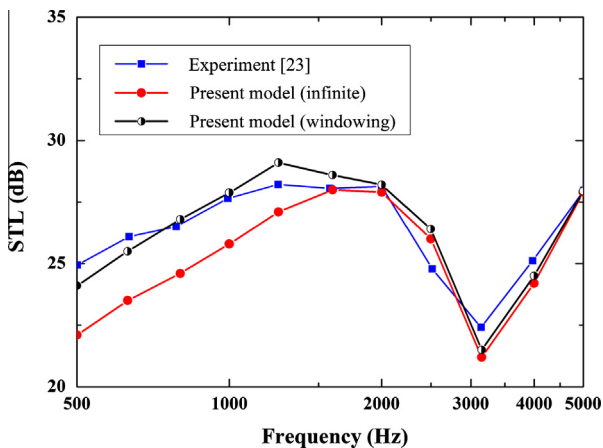


Fig. 3. Comparison between the present model predictions and the experimental results [23] for sound transmission loss (1/3 octave) of unidirectional stiffened plate.

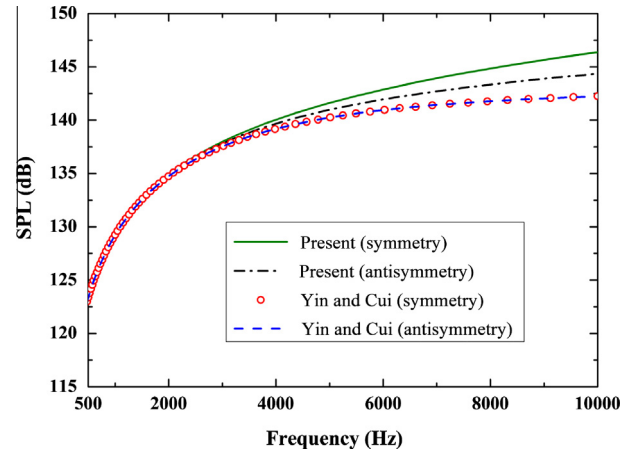


Fig. 4. Comparison between present predictions and those of Yin and Cui [24] for symmetric and antisymmetric laminated schemes under a transverse point force excitation.

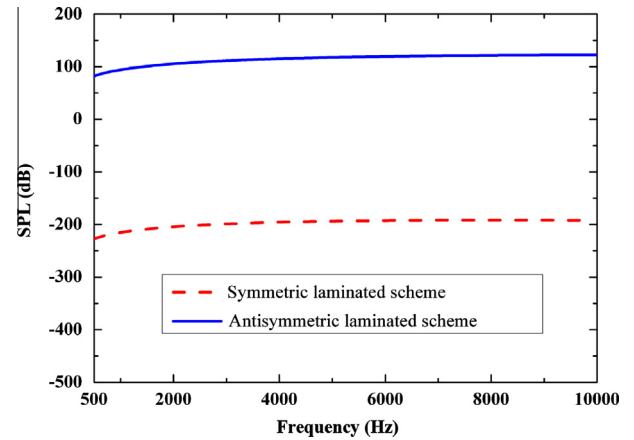


Fig. 5. Comparison between symmetrical and anti-symmetrical laminated schemes under unit point in-plane force excitation.

effect, the anti-symmetric plate can radiate much larger sound pressure compared to the symmetric one. Notice that, for in-plane force excitation, the flexural-extension coupling effect may be maximized because it is exactly this kind of coupling effect that converts longitudinal wave energy to bending wave energy. The results of Figs. 4 and 5 reveal that the SPL of a composite plate excited by unit in-plane force is much lower than that of a composite plate excited by unit transverse point force. This implies that the contribution from in-plane force excitation to radiation power may be neglected in comparison with that from transverse force excitation of the same amplitude.

3.3. Flexural-torsion coupling effect of composite bare plate

The flexural-torsion coupling effect has been found to be important in designing forward-swept wing composite structures having enhanced aerodynamic performance [26]. How such coupling effect affects the vibroacoustic behaviors of a composite plate is therefore of significant interest but always unnoticed by previous researchers. To avoid the influence of other coupling effects, three symmetric schemes are selected, including single-layer configuration ($[45^\circ/45^\circ/45^\circ]$), regular symmetric angle-ply configuration with three layers $[45^\circ/-45^\circ/45^\circ]$ and fifteen layers $[45^\circ/-45^\circ/45^\circ/-45^\circ/45^\circ/-45^\circ/45^\circ/-45^\circ/45^\circ/-45^\circ]_{\text{sym}}$. The predictions are presented in Fig. 6. Notice that, the single layer configuration

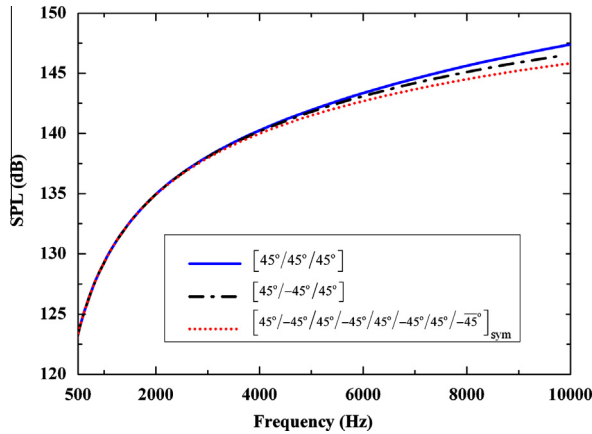


Fig. 6. Influence of flexural-torsion coupling effect upon SPL versus frequency curve of symmetric composite plates.

means one scheme with flexural-torsion coupling effect, and this coupling effect decreases as the number of layers is increased for symmetric angle-ply configurations.

The results of Fig. 6 shows that the single layer configuration produces larger far-field pressure over the other two symmetric laminate schemes considered, which is consistent with existing results [27]. This is because the flexural-torsion coupling effect can enlarge the bending deformation under transverse loading. The observed discrepancy between single layer configuration and multi-layer configurations illustrates the necessity for considering the flexural-torsion coupling effect especially in the high frequency regime.

3.4. Flexural-torsion coupling effect of stiffeners

Whilst it has been well established that flexural-torsion coupling is important for beam structures with channel cross sections, it is yet unclear to what extent this coupling effect may affect the vibroacoustic response of a stiffened plate as such effect is usually neglected for simplicity [23]. Fig. 7 plots the predicted far field pressure of single layer [45°] configuration excited by unit transverse point force, with and without considering the flexural-torsion coupling of the stiffeners. The results without flexural-torsion coupling are obtained by neglecting the torsion motion

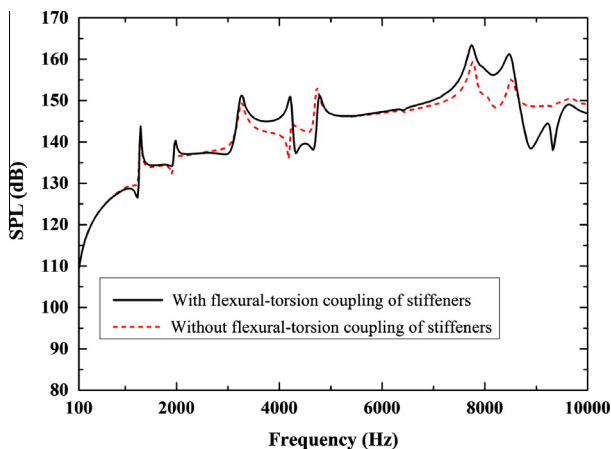


Fig. 7. Predictions with and without considering flexural-torsion coupling effect of stiffeners for single layer configuration.

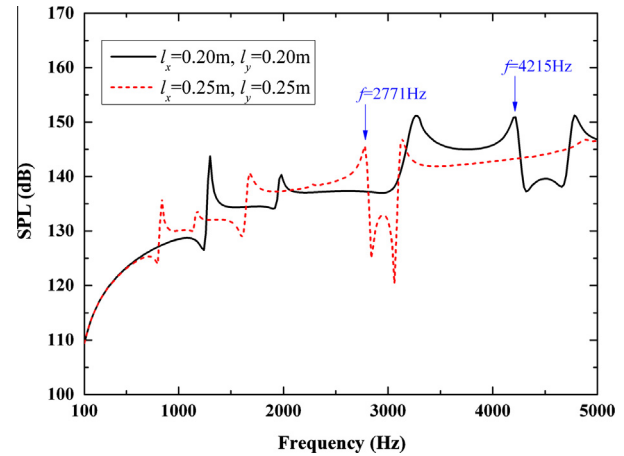


Fig. 8. Influence of periodical spacing on sound radiation of the structure.

equations and coupling coefficient χ_x in Eq. (15). As shown in Fig. 7, the flexural-torsion coupling effect of the stiffeners affects the tendency of the SPL curve of the structure mainly in the way of changing the peaks and dips in the SPL curve especially in higher frequency range. As a matter of fact, this proves the importance and necessity of the accurate stiffener modeling.

3.5. Influence of stiffener spacings

As the stiffener spacing (l_x, l_y) is one of the most important geometric parameters governing wave propagation in the whole structure, it is of great significance to evaluate its influence on sound radiation characteristic of the structure. Fig. 8 illustrates the far field radiated sound pressure with (l_x, l_y) selected as (0.2, 0.2)m and (0.25, 0.25)m respectively.

The attractive phenomena on the results is that all the peaks and dips on the curve shift to lower frequency as the stiffener spacings are increased. In fact, the inter-stiffener panels can be treated as small bounded plates approximately as stated by Fahy and Gardonio [25], and the peaks or dips on the radiation curves correspond to resonance frequencies of these bounded plates. Therefore, larger spacing results in lower natural frequency for fixed mode order. Moreover, the approximate quantitative relation $4215/2771 \approx (25/20)^2$ for two peaks as shown in the figure confirms the present explanation again.

4. Conclusions

In this study, a layerwise shear deformable theory is adopted to develop an analytical model for describing the vibroacoustic of orthogonally stiffened laminated composite plates, in which full account is given to various coupling effects including the flexural-extension and the flexural-torsion couplings of the composite base plates. Numerical results show that the coupling effects (i.e., the flexural-extension and the flexural-torsion couplings) owing to material anisotropic base plate and the geometrical anisotropic stiffeners can both play a significant influence on structure sound radiation, which are also influenced by specific material properties, lamination schemes and excitation frequencies etc. Particularly, the symmetry of the composite plate exerts a significant effect on the sound radiation of the considered structure when excited by an in-plane point force. Moreover, since the inter-stiffener panels can be treated as small bounded plates, the increase of the stiffener spacing leads to the decrease of the natural frequency of the structure for fixed mode order.

Acknowledgements

This work is supported by the National Basic Research Program of China (2011CB6103005), the National Natural Science Foundation of China (11102148, 11072188 and 11021202), and the Fundamental Research Funds for Central Universities (xjj2011005).

References

- [1] Zhao J, Wang XM, Chang JM, Yao Y, Cui Q. Sound insulation property of wood-waste tire rubber composite. *Compos Sci Technol* 2010;70(14):2033–8.
- [2] Langley RS. A dynamic stiffness technique for the vibration analysis of stiffened shell structures. *J Sound Vib* 1992;156(3):521–40.
- [3] Mead DJ, Pujara KK. Space-harmonic analysis of periodically supported beams: response to convected random loading. *J Sound Vib* 1971;14(4):525–32.
- [4] Langley RS, Heron KH. Elastic wave transmission through plate beam junctions. *J Sound Vib* 1990;143(2):241–53.
- [5] Wang J, Lu TJ, Woodhouse J, Langley RS, Evans J. Sound transmission through lightweight double-leaf partitions: theoretical modelling. *J Sound Vib* 2005;286(4–5):817–47.
- [6] Xin FX, Lu TJ. Sound radiation of orthogonally rib-stiffened sandwich structures with cavity absorption. *Compos Sci Technol* 2010;70(15):2198–206.
- [7] Xin FX, Lu TJ. Analytical modeling of fluid loaded orthogonally rib-stiffened sandwich structures: sound transmission. *J Mech Phys Solids* 2010;58(9):1374–96.
- [8] Maxit L. Wavenumber space and physical space responses of a periodically ribbed plate to a point drive: a discrete approach. *Appl Acoust* 2009;70(4):563–78.
- [9] Mace BR. Sound radiation from a plate reinforced by two sets of parallel stiffeners. *J Sound Vib* 1980;71(3):435–41.
- [10] Mace BR. Sound radiation from fluid loaded orthogonally stiffened plates. *J Sound Vib* 1981;79(3):439–52.
- [11] Takahashi D. Sound radiation from periodically connected double-plate structures. *J Sound Vib* 1983;90(4):541–57.
- [12] Yin X, Gu X, Cui H, Shen R. Acoustic radiation from a laminated composite plate reinforced by doubly periodic parallel stiffeners. *J Sound Vib* 2007;306(3–5):877–89.
- [13] Legault J, Mejdi A, Atalla N. Vibro-acoustic response of orthogonally stiffened panels: the effects of finite dimensions. *J Sound Vib* 2011;330(24):5928–48.
- [14] Mejdi A, Legault J, Atalla N. Transmission loss of periodically stiffened laminate composite panels: shear deformation and in-plane interaction effects. *J Acoust Soc Am* 2012;131(1):174–85.
- [15] Ghinet S, Atalla N. Modeling thick composite laminate and sandwich structures with linear viscoelastic damping. *Comput Struct* 2011;89(15):1547–61.
- [16] Librescu L, Song O. Thin-walled composite beams: theory and application. Springer; 2006. p. 107.
- [17] Lee J, Kim SE. Flexural-torsional coupled vibration of thin-walled composite beams with channel sections. *Comput Struct* 2002;80(2):133–44.
- [18] Xin FX, Lu TJ. Transmission loss of orthogonally rib-stiffened double-panel structures with cavity absorption. *J Acoust Soc Am* 2011;129:1919–34.
- [19] Junger MC, Feit D. Sound, structures, and their interaction. 2nd ed. MIT Press; 1986. p. 100–3.
- [20] Brunskog J, Hammer P. Prediction model for the impact sound level of lightweight floors. *Acta Acust United Acust* 2003;89(2):309–22.
- [21] Villot M, Guigou C, Gagliardini L. Predicting the acoustical radiation of finite size multi-layered structures by applying spatial windowing on infinite structures. *J Sound Vib* 2001;245(3):433–55.
- [22] Rhazi D, Atalla N. A simple method to account for size effects in the transfer matrix method. *J Acoust Soc Am* 2010;127(2). EL30–6.
- [23] Guigou-Carter C, Villot M. Modelling of sound transmission through lightweight elements with stiffeners. *Build Acoust* 2003;10(3):193–209.
- [24] Yin X, Cui H. Acoustic radiation from a laminated composite plate excited by longitudinal and transverse mechanical drives. *J Appl Mech-T ASME* 2009;76:044501.
- [25] Fahy F, Gardonio P. Sound and structural vibration: radiation, transmission and response. 2nd ed. Academic Press; 2007. p. 243–30.
- [26] Jones RM. Mechanics of composite materials. 2nd ed. Taylor & Francis Group; 1999. p. 211.
- [27] Zhang CZ. General analytic solutions for transverse bending of general ply composite rectangular thin plate. *Struct Environ Eng* 1998;4:39–48 [in Chinese].